Optically pumped InGaN/GaN lasers with wet-etched facets

D. A. Stocker[a)] and E. F. Schubert
Center for Photonics Research, Boston University, Boston, Massachusetts 02215

J. M. Redwing
Epitronics, Phoenix, Arizona 85027

(Received 3 December 1999; accepted for publication 30 October 2000)

Optically pumped laser action is demonstrated in InGaN/GaN double heterostructure lasers with wet-etched facets. The facets are formed by a two-step etching process which creates vertical facets with less than 5 nm roughness. The first step, photoenhanced electrochemical wet etching, is used to define the laser cavities. The second step reduces the facet roughness by crystallographic wet chemical etching. Lasing is demonstrated by an increase in the differential quantum efficiency, linewidth narrowing, and strongly polarized output above threshold. The threshold varies with cavity length from 2.4 MW/cm^2 for 500 μm cavities to 23 MW/cm^2 for 50 μm cavities. A modal loss of 15 cm^{-1} is deduced from an analysis of the threshold pumping power as a function of cavity length. © *2000 American Institute of Physics.* [S0003-6951(00)00852-4]

Facets for GaN-based lasers are typically fabricated by cleaving[1–5] or dry etching techniques.[6–8] Cleaved facets of InGaN/GaN lasers grown on sapphire substrates have stepped or striated surfaces,[9] although atomically smooth surfaces are possible for GaN grown on spinel,[3] SiC,[5] and GaN substrates.[2] Dry etching techniques have been shown to produce facets with a rms roughness as low as 5 nm.[6] Photoenhanced electrochemical etching of GaN has also been reported, but the sidewalls produced using this method are generally too rough to be used as laser facets.[10–12] We present wet-etched GaN-based laser structures with smooth facets: Photoenhanced electrochemical (PEC) wet etching is used to define the lengths of the laser bars, and the roughness of the PEC-etched facets is greatly reduced by subsequent crystallographic etching. This crystallographic wet chemical etching technique produces vertical sidewalls with a rms roughness less than 5 nm.[13]

The InGaN/GaN double-heterostructure lasers were prepared as follows: After an initial 10-μm-thick buffer layer of GaN was grown on c-plane sapphire by hydride vapor phase epitaxy, a 0.5 μm GaN bottom cladding layer, a 1000 Å $In_{0.09}Ga_{0.91}N$:Si active region, and a 2200 Å GaN top cladding layer were grown by metalorganic vapor phase epitaxy. The double heterostructure is a single-mode waveguide with an active region confinement factor $\Gamma = 0.06$, as determined by slab waveguide calculations.

180-nm-thick Ni masks annealed at 650 °C for 2 min in a N_2 ambient were used to define cavities with lengths varying from 50 to 500 μm. The edges of the masks were aligned with the $\langle 11\bar{2}0 \rangle$ direction of the GaN, so that the resulting PEC-etched sidewalls corresponded to the $\{10\bar{1}0\}$ plane for subsequent crystallographic etching.

The samples were PEC etched in a 0.03 M KOH solution at room temperature with a bias voltage. During etching, the samples were clamped against a nickel bar and immersed along with a gold wire cathode in the aqueous KOH solution. A direct current power source supplied a 2 V bias between anode and cathode. A 200 W Hg vapor lamp with collimating optics provided a 1 cm^2 beam of ultraviolet illumination, and a silicon wafer was used as a cold mirror to reduce heating by increasing the ratio of UV to IR illumination.[14] Introduction of the cold mirror did not affect the etch rate significantly, and no etching was observed without UV illumination. PEC etching was monitored by periodically blocking the light and observing the change in current density. The change in current density was approximately 2 mA/cm^2 initially, and this value gradually decreased as the etch proceeded. The time required to produce vertical sidewalls extending down to the sapphire substrate under these conditions was 4 h.

A typical PEC-etched InGaN/GaN sidewall is shown in Fig. 1(a). The nickel mask is visible at the top of the image; the mask was allowed to remain in place throughout the

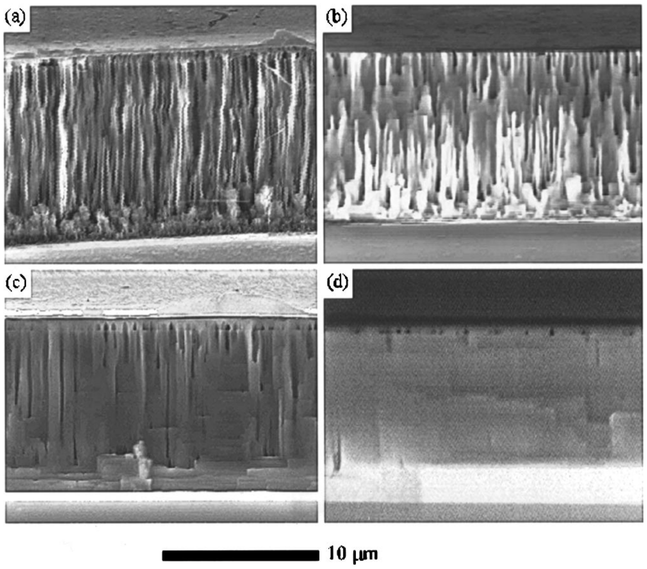

FIG. 1. Smoothing of a vertical sidewall produced by PEC etching of an InGaN/GaN double heterostructure. The 10 μm bar applies to all SEM images. (a) PEC-etched facet. (b)–(d) Facets after crystallographic etching in molten KOH at 175 °C for (b) 1, (c) 3, and (d) 9 min.

[a)] Electronic mail: dstocker@draper.com subsequent crystallographic etching. As the image shows, the PEC-etched sidewall is extremely rough and has a fibrous texture, although the lower GaN surface has etched away cleanly from the sapphire substrate. From scanning electron microscope (SEM) images we estimate a rms roughness for the PEC-etched facets of 200–300 nm.[15] Note that there are some deep holes in the top 1 μm of the structure, near the InGaN layer. These holes formed during PEC etching, but the etching mechanism is not yet fully understood.

The sidewall produced by PEC etching was too rough to be used as a laser facet, since the reflectivity decreases with increasing surface roughness.[9] If crystallographic etching of GaN behaves similarly to that of GaAs,[16] then in some solvents the gallium-terminated surface should etch more slowly than the nitrogen-terminated surface and planes that are mixed, i.e., partially nitrogen and partially gallium terminated, should have etch rates that fall between the two extremes. The slower-etching surfaces (0001) and $\{10\bar{1}0\}$ become smooth during etching. This was exploited by etching in molten KOH to smooth the PEC-etched surface.

The series of SEM images in Figs. 1(b)–1(d) shows the effect that etching in 175 °C molten KOH has on the sidewall. The etch rate at this temperature was approximately 0.05 μm/min. The fibrous PEC-etched surface showed considerable smoothing after only 1 min of crystallographic etching, as can be seen in Fig. 1(b). Further improvement is observed in Fig. 1(c) after 3 min of crystallographic etching. After 5 min of etching, no further smoothing occurred; the image shown in Fig. 1(d) after 9 min of etching is very similar to images taken anywhere in the range of 5–10 min. Note that the density of holes in the top 1 μm did not tend to change during crystallographic etching. Horizontal steps like those across the center of Fig. 1(d) are common features produced by crystallographic etching in KOH. These may be due to etch rate anisotropy in the [0001] and $[000\bar{1}]$ directions. The lateral dimension of the smooth areas before a step occurs is on the order of 10 μm.

Before optical pumping, the nickel mask was removed by wet etching in a 1 HCl:1 HNO_3:3 H_2O solution for 30 min. A nitrogen laser emitting at 337.1 nm was used to pump a 200 μm wide region of the cavity. This laser provided a pulse width of 800 ps and a maximum power density of 98 MW/cm^2. Neutral density filters were used to attenuate the pumping power.

Several spectra for a 500 μm wet-etched cavity are shown in Fig. 2. Below the threshold pumping power a broad band is visible at 3.18 eV (390 nm). Near the 2.7 MW/cm^2 threshold pumping power density a narrow peak appears at 3.13 eV (396 nm). As the pumping power was increased the peak continued to narrow and also shifted to a slightly lower energy. The decrease in the full width at half maximum (FWHM) and the increase in the differential quantum efficiency indicate stimulated emission, but not necessarily laser oscillation. Laser oscillation is verified by an increase in the ratio of the TE to TM mode intensities. A plot of the peak emission intensity, FWHM, and TE/TM ratio for a 500 μm cavity is shown in Fig. 3. A sharp decrease in the FWHM from ~100 meV to less than kT, an increase in differential quantum efficiency, and an increase of the TE/TM ratio occur concurrently at the 2.7 MW/cm^2 threshold density. The laser modes could not be resolved due to pulse-to-pulse amplitude noise of the excitation source.

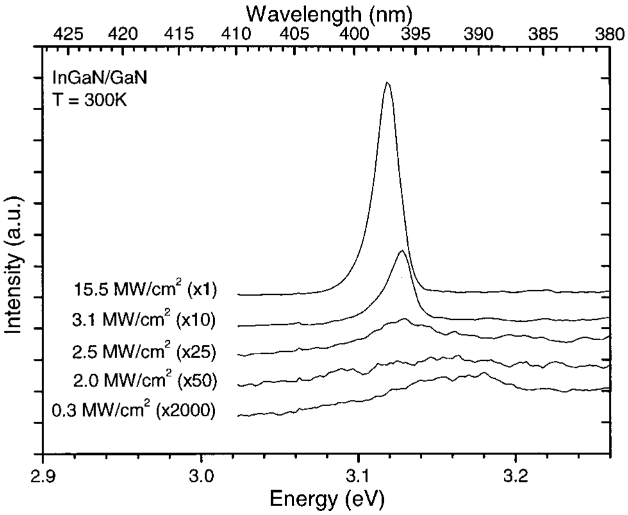

FIG. 2. Emission spectra of a 500 μm wet-etched laser cavity for several different pumping power levels at room temperature. At subthreshold excitation powers, a broad band appears at 3.18 eV (390 nm). Above threshold, a narrow peak emerges at 3.13 eV (396 nm) and shifts to slightly lower energies as pumping power is increased.

Threshold pumping power densities on the order of MW/cm^2 are common for optically pumped III–V nitride structures.[17–19] It should also be noted that the power density exciting the active region was lower than the incident power density due to inefficient diffusive transport through the 2200 Å top cladding layer.

At threshold, the round-trip net gain in the cavity is unity. For a cavity with two identical mirrors, this means that the increase in intensity gained by one pass through the active region is exactly offset by the decrease in intensity upon reflection at one of the facets. That is

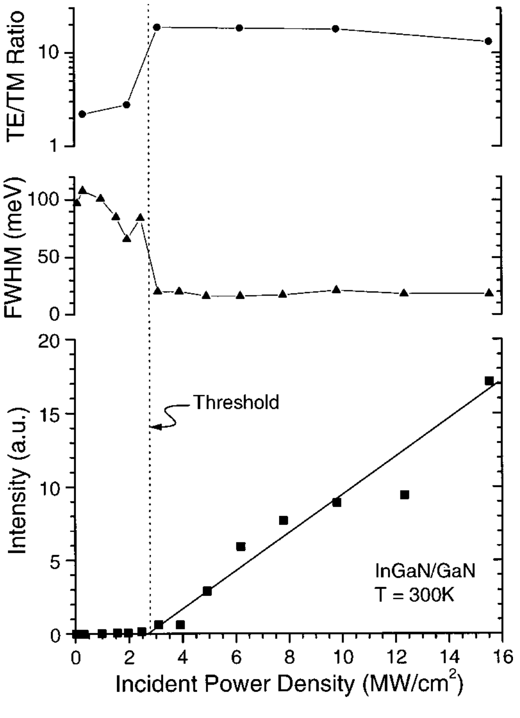

FIG. 3. Peak emission intensity, FWHM, and TE/TM ratio for a 500 μm wet-etched laser cavity over a wide range of pumping power densities. The laser threshold is 2.7 MW/cm^2.

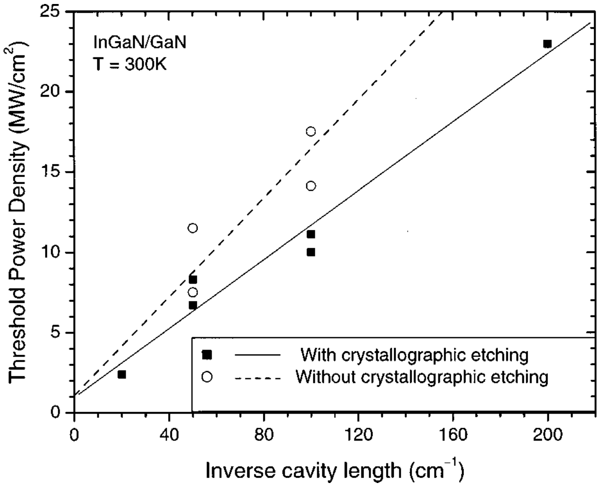

FIG. 4. Threshold power density as a function of inverse cavity length for PEC-etched cavities with and without smoothing by crystallographic wet etching. The solid and dashed lines are fitted to the points for cavities with and without crystallographic etching, respectively.

$$e^{(g-\alpha)L} = 1/R, \tag{1}$$

where g is the modal gain, α is the modal loss coefficient, L is the cavity length, and R is the reflectivity of the facet. Rearranging this equation yields

$$g|_{\text{at threshold}} = \alpha - \ln(R)/L. \tag{2}$$

This straight-line plot of gain versus inverse cavity length is realized in Fig. 4, with the assumption that the linear gain model holds. The solid squares indicate the threshold pumping power densities for PEC-etched facets after crystallographic etching. Assuming a reflectivity near the ideal value of 0.2 for the crystallographically etched facets, which is reasonable for a facet roughness less than 5 nm,[9] the modal loss in the material is $\sim 15\,\text{cm}^{-1}$, which is a typical value for this materials system.[20]

Two points each for 200 and 100 μm cavities that were made by PEC etching without subsequent crystallographic etching have also been added to Fig. 4 (the hollow circles). The linear fit for the PEC-etched cavities is constrained to cross the y axis at the same point as the line for crystallographically etched cavities. This constraint is equivalent to requiring that the threshold be the same for infinitely long cavities with different, nonzero facet reflectivities. For an infinitely long cavity, the threshold optical gain is equal to the loss, independent of the reflectivity, as can be inferred from Eq. (2). A comparison of the two linear fits reveals that the threshold is lower after crystallographic etching.

We attribute this decrease to an increase in the facet reflectivity. Comparing the linear fits for the cavities with and without crystallographic etching indicates that the power reflectivity increases by a factor of 2 as a result of smoothing. This estimate is conservative: if the reflectivity of the crystallographically etched facets were lower than the assumed ideal value of 0.2, then the increase in reflectivity as a result of smoothing would be even more dramatic.

In conclusion, we have presented InGaN/GaN lasers with wet-etched facets. The facets are fabricated using a two-step etching process. In the first step, the laser cavity length is defined by PEC etching. The facet roughness resulting from PEC etching is reduced by the second, crystallographic etching step. Crystallographic etching increases the reflectivity by at least a factor of 2. The threshold power densities for the wet-etched lasers vary monotonically with the length of the cavities, from $2.4\,\text{MW/cm}^2$ for 500 μm cavities to $23\,\text{MW/cm}^2$ for 50 μm cavities. A modal loss of $15\,\text{cm}^{-1}$ is deduced from an analysis of the threshold pumping power as a function of cavity length.

The authors thank J. W. Graff for expert assistance in mask fabrication. Research at Boston University is supported in part by ONR (Dr. C. E. C. Wood) and NSF (Dr. R. P. Khosla). Support at Epitronics was provided by DARPA and the U.S. Army Missile Command under Contract No. DAAH01-96-C-R192.

[1] D. Stocker, E. F. Schubert, K. S. Boutros, J. S. Flynn, R. P. Vaudo, V. M. Phanse, and J. M. Redwing, Electron. Lett. **34**, 373 (1998).
[2] S. Nakamura *et al.*, Appl. Phys. Lett. **73**, 832 (1998).
[3] M. A. Khan, C. J. Sun, J. W. Yang, Q. Chen, B. W. Lim, M. Z. Anwar, A. Osinsky, and H. Temkin, Appl. Phys. Lett. **69**, 2418 (1996).
[4] S. Nakamura, M. Senoh, S. Nagahama, N. Iwasa, T. Yamada, T. Matsushita, T. Sugimoto, and H. Kiyoku, Appl. Phys. Lett. **69**, 1477 (1996).
[5] K. Doverspike *et al.*, Photonics West 1998 Conference.
[6] M. Kneissl, D. P. Bour, N. M. Johnson, L. T. Romano, B. S. Krusor, R. Donaldson, J. Walker, and C. Dunnrowicz, Appl. Phys. Lett. **72**, 1539 (1998).
[7] S. Nakamura, M. Senoh, S. Nagahama, N. Iwasa, T. Yamada, T. Matsushita, H. Kiyoku, and Y. Sugimoto, Jpn. J. Appl. Phys., Part 2 **35**, L74 (1996).
[8] F. Binet, J. Y. Doboz, N. Laurent, C. Bonnat, P. Collot, F. Hanauer, O. Briot, and R. L. Aulombard, Appl. Phys. Lett. **72**, 960 (1998).
[9] D. A. Stocker, E. F. Schubert, W. Grieshaber, K. S. Boutros, and J. M. Redwing, Appl. Phys. Lett. **73**, 1925 (1998).
[10] D. A. Stocker and E. F. Schubert, J. Electrochem. Soc. **146**, 2702 (1999).
[11] C. Youtsey, I. Adesida, L. T. Romano, and G. Bulman, Appl. Phys. Lett. **72**, 560 (1998).
[12] M. S. Minsky, M. White, and E. L. Hu, Appl. Phys. Lett. **68**, 1531 (1996).
[13] D. A. Stocker, E. F. Schubert, and J. M. Redwing, Appl. Phys. Lett. **73**, 2654 (1998).
[14] The index of refraction of Si varies between 5 and 7 in the spectral range from 300–400 nm and drops to less than 3.5 above 1000 nm. This causes the power reflectivity at a 45° incidence angle to vary from ~50% in the near UV to ~30% in the near IR. Thus, using the light reflected from the silicon wafer increases the ratio of UV to IR, allowing a relatively high etch rate while minimizing possible heating effects.
[15] Due to the geometry of the GaN/sapphire samples, attempts at determining the roughness by atomic force microscopy were unsuccessful.
[16] R. Williams, *Modern GaAs Processing Methods* (Artech House, Boston, 1990), p. 98.
[17] D. Hofstetter, R. L. Thornton, M. Kneissl, D. P. Bour, and C. Dunnrowicz, Appl. Phys. Lett. **73**, 1928 (1998).
[18] S. Bidnyk, B. D. Little, Y. H. Cho, J. Krasinski, J. J. Song, W. Yang, and S. A. McPherson, Appl. Phys. Lett. **73**, 2242 (1998).
[19] I. K. Shmagin, J. F. Muth, R. M. Kolbas, S. Krishnankutty, S. Keller, U. K. Mishra, and S. P. DenBaars, J. Appl. Phys. **81**, 2021 (1997).
[20] D. P. Bour *et al.*, IEEE J. Sel. Top. Quantum Electron. **4**, 498 (1998).